

Validation of selected *TESS* exoplanetary candidates

M. Mesarč¹  and Ľ. Hambálek² 

¹ *Department of Theoretical Physics and Astrophysics, Faculty of Science
 Masaryk University, Kotlářská 267/2, 611 37 Brno, Czech Republic*

² *Astronomical Institute of the Slovak Academy of Sciences
 059 60 Tatranská Lomnica, The Slovak Republic, (E-mail: lhambalek@ta3.sk)*

Received: October 30, 2023; Accepted: December 12, 2023

Abstract. We have selected suitable 6 exoplanetary candidates from the *TESS* database which were observable using a network of small ground-based telescopes to collect photometric transits during follow-up observation. We have made a new reduction of *TESS* photometry using a custom aperture, as well as reducing the ground-based aperture photometry. We have refined the period of transits and constructed $O - C$ diagrams. Mean transit was fitted in all observed photometric filters and we derived individual candidate's physical parameters. Using the colour indices during transit, we hint at the exoplanetary nature of candidates. Three targets TOI-1518b, TOI-2046b, and TOI-2109b were confirmed as exoplanets by other authors during the writing of this thesis. Here, we have provided an independent evaluation and analysis, without any knowledge of their results. TOI-3856.01 is among the targets more likely a substellar object based on my results, but it has not been confirmed yet. In the case of TOI-1834.01, we have proposed another scenario incompatible with the original assumption that it was an exoplanetary candidate and we assume that it is a hierarchical triple system. TOI-3604.01 was also modelled concerning parasitic light in the aperture. Individual models suggest a body too large for an exoplanet.

Key words: Planetary systems – Binaries: eclipsing – Techniques: photometric

1. Introduction

The Transiting Exoplanet Survey Satellite (*TESS*, Ricker et al., 2015) is a NASA space all-sky survey that continuously monitors strips of the sky for ~ 27 continuous days (i.e. sectors) alternating between the north and south hemispheres. The cadence of observation was at first 30 min, 2 min and later 20 s for selected targets. The detector bandpass spans from 600 – 1040 nm and is centred on the traditional Cousins I-band ($\lambda_{\text{eff}} = 786.5$ nm). The red part is preferred for increased sensitivity to small planets transiting in front of cool, red stars, but lacks the colour information of standard photometric filters.

We have selected six *TESS* objects of interest (TOIs) that were still considered candidates for exoplanets (see Tab. 1) in 2021. The selection criteria had

Table 1. Preliminary transit properties of target TOIs at the start of the campaign: host star magnitudes in *TESS* and *V* bands, normalized depth of transit ΔF , transit duration t_T , and period P .

TOI	1518.01	1834.01	2046.01	2109.01	3604.01	3856.01
<i>TESS</i> [mag]	8.75	11.50	11.00	9.79	11.73	11.66
<i>V</i> [mag]	8.95	12.15	11.55	10.22	12.51	12.29
ΔF [%]	0.98	2.11	1.47	0.67	1.49	1.29
t_T [h]	2.35	1.85	2.41	1.80	1.64	1.51
P [d]	1.90261	1.21681	1.49718	0.67249	1.06669	2.04345

to ensure observability in Central Europe (Dec > -10 deg), a higher occurrence of transits per night ($P < 2.2$ d, $t_T < 3$ h), and bright host stars ($V \leq 12.5$ mag) with deep transits ($\Delta F \geq 0.65\%$) enough for sub-metre telescopes. We planned the observation with TransitFinder (Jensen, 2013) and coordinated observers who were part of ETD (Poddaný et al., 2010), ExoClock (Kokori et al., 2022), and MuSCAT2 (Narita et al., 2019) projects (see Acknowledgements). This article is based on results of the master thesis by Mesarč (2023).

2. Reduction

The available *TESS* data of our targets covered 2–5 sectors per object during the September 2019 – December 2022 time frame. In total, 316 individual transits were identified. *TESS* data were reduced independently of the pipeline first by TPF (Target Pixel File) identification using Python package `lightkurve` (Lightkurve Collaboration et al., 2018) with custom pixel aperture for each TOI using `tpfplotter` (Aller et al., 2020). Each FOV was individually visually inspected for nearby transit-like variable signals in each pixel of the selected aperture and close vicinity. Individual sectors (with 20 s, 2 min, and 30 min cadence) were treated separately. Outliers were removed by Sigma clipping, transits were identified and incomplete ones were omitted for further analysis. For TOI-3856.01 we also had to correct for momentum dumps. Afterwards, our custom-mask flux was de-trended using `exoplanet` package (Foreman-Mackey et al., 2021).

Follow-up observations took part from May 2021 to April 2022. In total, 136 transits were observed at 27 sites with the help of 33 observers in the campaign. Telescopes with diameters 150–1520 mm were used. Various observers had different photometric passbands at their disposal: Johnson *BVRI*, Sloan *g'r'i'z'*, or filter-less clear or luminance band.

For the basic photometric reduction, the HOPS software (Tsiaras, 2019) was used. This allowed for the use of multiple check stars with a circular aperture automatically determined by the stellar FWHM. In each field, we have selected

Table 2. Comparison of our results to those models from papers published during the preparation of the master thesis. Individual papers are: C21 = Cabot et al. (2021), K22 = Kabáth et al. (2022), and W21 = Wong et al. (2021).

Parameter	TOI-1518b		TOI-2046b		TOI-2109b	
	This work	C21	This work	K22	This work	W21
R_P/R_S	0.0819(6)	0.0816(2)	0.1173(8)	0.1213(19)	0.1022(20)	0.0988(13)
a/R_S	2.14(1)	2.27(2)	4.53(5)	4.75(18)	4.13(1)	4.29(1)
b	0.785(6)	0.748(7)	0.60(2)	0.51(6)	0.882(6)	0.904(6)
i [deg]	68.9(3)	70.7(4)	81.8(3)	83.6(9)	77.7(2)	77.8(2)
t_T [h]	2.070(12)	1.801(13)	2.591(10)	2.410(31)	2.395(18)	2.347(8)
ρ_* [g cm ⁻³]	0.417(50)	0.417(55)	0.859(101)	0.890(98)	0.341(56)	–
ΔF [%]	0.667(6)	0.665(4)	1.476(18)	1.627(9)	1.044(16)	0.976(8)

4–7 check stars so that they show no signs of variability. A standard dark and flat calibration of all frames was performed. From the check stars available in each FOV, an artificial star was constructed to do the relative aperture photometry.

3. Modelling of transits

The total de-trended *TESS* light curve (LC) was analysed with a box-fitting least-square algorithm by Kovács et al. (2002) to find period P and starting epoch T_0 for the transit ephemeris. This was used to predict follow-up ground-based observations. We have constructed the phased *TESS* LC and selected the region ± 4 hours around the mid-transit.

Using the mean transit shape, we were able to find more precise times of mid-transit for 30-minute *TESS* cadence even when each transit was covered by only a handful of points. The data was used to construct an $O - C$ diagram.

TESS transit model was calculated using the `pyaneti` code by Barragán et al. (2019). The code utilises the MCMC method to compute transit parameters: the planet-star radius ratio R_P/R_S , the ratio of the semi-major axis to the stellar radius a/R_S , inclination i of the orbital plane (or the impact parameter b), duration t_T . The limb-darkening coefficients were adopted using a parametrization proposed by Kipping (2013).

The ground-based transits were modelled by the `HOPS` package (Tsiaras et al., 2016). The necessary stellar limb-darkening coefficients were calculated with the `ExoTETHys` package (Morello et al., 2020) for each passband using the non-linear law by Claret (2000) and the stellar parameters were taken from NASA Exoplanet Archive.

Table 3. Our results of assumed exoplanet transit models of TOIs without known paper published before May 2023. Note: for TOI-3604.01, model A treats all light as a single star in *TESS* pixel, while model B assumes half of the observed flux as contamination.

Parameter	TOI-1834.01	TOI-3604.01		TOI-3856.01
		A	B	
R_P/R_S	0.1485(59)	0.1219(20)	0.1599(7)	0.1135(24)
a/R_S	3.25(6)	4.38(8)	5.50(3)	6.13(22)
b		0.891(9)	0.724(49)	0.818(26)
i [deg]	74.1(4)	81.0(5)	86.5(9)	82.3(5)
t_T [h]	2.178(27)	1.689(15)	1.715(9)	1.942(40)
ρ_* [g cm ⁻³]	1.332(162)	1.407(360)	1.407(360)	0.957(201)
ΔF [%]	2.206(37)	1.585(40)	2.556(28)	1.289(13)

4. Results

Since the *TESS* detector has 21-arcsec pixel scale (see Ricker et al., 2015), we had to check if there are more light sources at the target TOIs position below this resolution. We have used publicly available speckle polarimetry from SAI 2.5-m telescope (Safonov et al., 2017), Alopeke Speckle Instrument at Gemini-North telescope (Howell et al., 2016; Howell & Furlan, 2022), and PHARO instrument at Palomar 5-m telescope (Hayward et al., 2001) of angular resolution in range of 20-89 mas. Only in the case of TOI 3604.01, there was a visible detection of another source within 0.3 arcsec off the target.

Some transit parameters from independent modelling of confirmed exoplanets during this work are listed in Tab. 2 and as of date non-confirmed candidates are in Tab. 3. We have additionally revised the linear ephemerides (Tab. 4) by incorporating every observed minimum.

Ground-based observations taken in different filters were analyzed separately. Parameters R_P/R_S , a/R_S , and i were found for each passband. The relation between R_P/R_S and λ_{eff} of filter shows “jumps” similar to rigorous models (see e.g. Fortney et al., 2010). TOI-1834.01 is an exception to this, which seems to have a monotonous function $R_P/R_S \propto \lambda_{\text{eff}}$ but only from $VR + r'i'$ passbands. It is also the only system with a periodic $O - C$ signal, with ~ 10 -min amplitude and a period of 80.3501 ± 0.3149 days.

Our multi-colour ground-based photometry allowed us to construct a differential colour transit LC. While no sufficiently precise spectroscopy was available for us, we still wanted to limit the possibility of false detection by investigating the limb-darkening profile of the transiting body. If the second component is a star on an inclined orbit, it would produce shallow grazing eclipses. However, a star has a different limb-darkening profile than an exoplanet with a night side facing the observer. According to Tingley (2004), exoplanetary transits produce

a double-horned profile in differential colour transit LC while a close binary shows no such feature.

Only a handful of our ground-based transits were observed in two or more filters during a single night. We have constructed a model LC for each colour. Then, by subtracting any two models we created an artificial colour LC in arbitrary phases to cover the full transit. The more distant the effective wavelength of bands, the higher the signal.

Table 4. Updated periods (P) and reference time of primary transit (T_0).

Object	T_0 [BJD _{TDB}]	P [d]
TOI-1518b	2459854.414430(41)	1.90261125(9)
TOI-1834.01	2458928.271637(210)	1.21644035(28)
TOI-2046b	2459883.844897(58)	1.49718679(15)
TOI-2109b	2459718.730971(82)	0.67247386(17)
TOI-3604.01	2459825.953340(850)	1.0666837(427)
TOI-3856.01	2459609.405178(2180)	2.04360450(119)

We have used all identified transits from *TESS* as well as ground-based follow-up to construct the $O - C$ diagram. Except for TOI-1834.01 (Fig. 1), no other target shows a meaningful signal. The most notable part of $O - C$ is taken during *TESS* sector 49 (February 26 – March 26, 2022). We have modelled this part and the whole $O - C$ using the code *OCFit* by Gajdoš & Parimucha (2019). We have fitted a simple 3-body scenario with MCMC resulting in $P_3 = 80.35013 \pm 0.31488$ d on a short ($a_3 \sin i_3 = 1.161 \pm 0.157$ au) eccentric ($e_3 = 0.265 \pm 0.135$) orbit. It is a similar solution to that of Czavalinga et al. (2023) which was published shortly before submitting the thesis. The problem is that considering the total $O - C$ amplitude is caused solely by LITE leads to unrealistic large mass function $f(m) = 32.33 M_\odot$.

We have also tried to model the transit of TOI-1834.01 as a grazing binary with the code *RMF* by Garai et al. (2020). The simplest case was to assume $M_2/M_1 = R_2/R_1$ and fit a model spectrum to the spectral energy distribution fixed around VizieR photometry. The best-fitting temperature was 5200 K corresponding to K0 spectral type or $\sim 0.79 M_\odot$, $\sim 0.85 R_\odot$ (based on tables by Cox (2000)). We can use equations 8 and 12 from Borkovits et al. (2016) to estimate amplitudes of LTTE and dynamical effects (for $M_1 = M_2 = M_3$) as $\mathcal{A}_{LTTE} = 78.68$ s and $\mathcal{A}_{dyn} = 567.38$ s, respectively. This is already enough to explain the observed 10-minute amplitude of $O - C$.

TOI-3604.01 is the only target resolved by speckle interferometry in near-IR into two sources of similar apparent luminosity separated by 0.3 arcsec. We have thus removed a constant 50% of total *TESS* out-of-transit flux and constructed a new model (B in Tab. 3) from the normalized treated flux. In this case, the supposed exoplanet orbiting one of the two stars had to be $\sim 30\%$ larger than

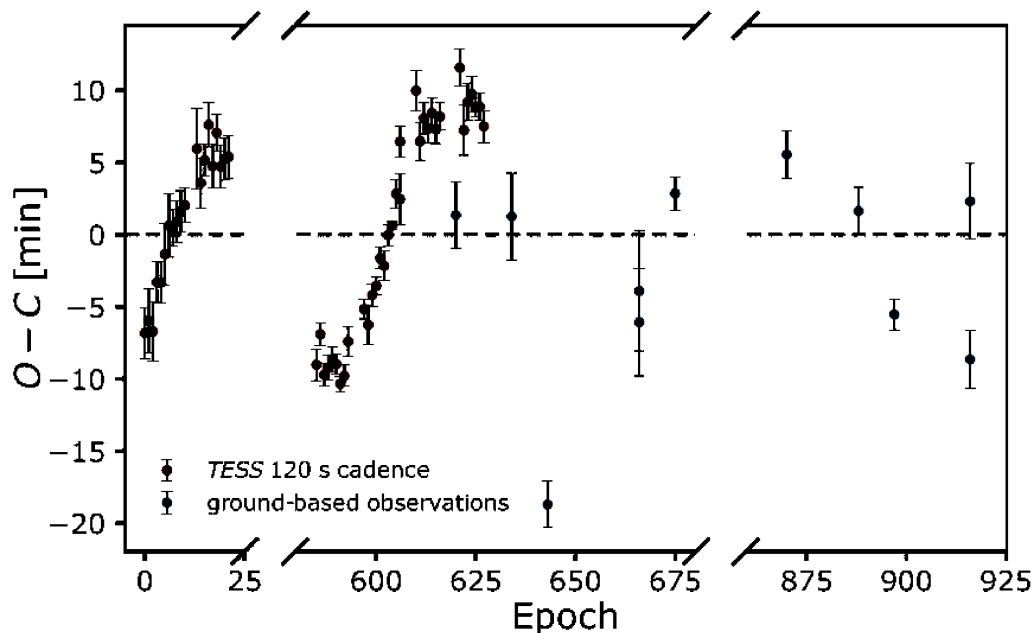


Figure 1. The $O - C$ diagram for TOI-1834.01 constructed with the updated ephemeris $T_0 = 2458925.271637 + 1.21644035 \times E$.

initially assumed, making it more likely to be a low-mass star. The parent object is also a very active red dwarf. Lambert et al. (2023) found maybe a similar (by R_P/R_S) object TOI-5375.01 which hosts a brown dwarf/low-mass star at hydrogen-burning limit with $\sim 83.8 \pm 2.1 M_J$.

TOI-3856.01 was at the time of this work not independently analyzed. The transit model based on ground photometry gives $R_P/R_S \in [0.112, 0.128]$ in seven different passbands (c.f. with Tab. 3). With stellar radius $R_\star = 1.12864 R_\odot$ (taken from the EXOFOP page), this gives the candidate radius as $R_P \in [1.26, 1.44] R_J$. The U-shaped single colour transits and double-horned differential colour transit suggest this object may be a hot Jupiter on ~ 0.034 au orbit.

5. Conclusion

We have selected six exoplanetary candidates as indicated by the *TESS* pipeline. From *TESS* photometry, we modelled their transits and got independent solutions for TOIs 1518b, 2046b, and 2109b. The TOI-1834.01 was independently found to be most probably a hierarchical triple star system of late K-type stars. Based on the corrected flux in *TESS* aperture, we found TOI-3604.01 to be probably a very low-mass star close to the hydrogen-burning limit. Based on our analysis, TOI-3856.01 appears to be a sub-stellar object.

Acknowledgements. This work was supported by the Slovak Research and Development Agency under the contract No. APVV-20-0148. This work has also been supported by the VEGA grant of the Slovak Academy of Sciences No. 2/0031/22. Thanks to all observers: Reinhold Friedrich Auer, Paul Benni, Giorgio Bianciardi, Matteo Cataneo, Giuseppe Conzo, Yannic Delisle, Vojtěch Dienstbier, Tommaso Dittadi, Frank Dubois, Gareb Enoc Fernández, Zoltán Garai, Snævarr Gudmundson, Veli-Pekka Hentunen, Yves Jongen, Taiki Kagitani, Peter Klagyivik, Felipe Murgas, Andre Kovacs, Hana Kučáková, Jean Claude Mario, Zlatko Orbanić, Ivo Peretto, Karol Petrík, Theodor Pribulla, Manfred Raetz, Roy René, Mark Salisbury, Sergei Shugarov, Pieter Vuylsteke, Noriharu Watanabe, Anaël Wünsche, and Miloslav Zejda.

References

- Aller, A., Lillo-Box, J., Jones, D., Miranda, L. F., & Barceló Forteza, S., Planetary nebulae seen with TESS: Discovery of new binary central star candidates from Cycle 1. 2020, *Astronomy and Astrophysics*, **635**, A128, DOI: 10.1051/0004-6361/201937118
- Barragán, O., Gandolfi, D., & Antoniciello, G., PYANETI: a fast and powerful software suite for multiplanet radial velocity and transit fitting. 2019, *Monthly Notices of the RAS*, **482**, 1017, DOI: 10.1093/mnras/sty2472
- Borkovits, T., Hajdu, T., Sztakovics, J., et al., A comprehensive study of the Kepler triples via eclipse timing. 2016, *Monthly Notices of the RAS*, **455**, 4136, DOI: 10.1093/mnras/stv2530
- Cabot, S. H. C., Bello-Arufe, A., Mendonça, J. M., et al., TOI-1518b: A Misaligned Ultra-hot Jupiter with Iron in Its Atmosphere. 2021, *Astronomical Journal*, **162**, 218, DOI: 10.3847/1538-3881/ac1ba3
- Claret, A., A new non-linear limb-darkening law for LTE stellar atmosphere models. Calculations for $-5.0 \leq \log[M/H] \leq +1$, $2000 \text{ K} \leq T_{\text{eff}} \leq 50000 \text{ K}$ at several surface gravities. 2000, *Astronomy and Astrophysics*, **363**, 1081
- Cox, A. N. 2000, *Allen's astrophysical quantities* (Springer New York, NY)
- Czavalinga, D. R., Borkovits, T., Mitnyan, T., Rappaport, S. A., & Pál, A., "Four new compact triply eclipsing triples found with Gaia and TESS. 2023, *Monthly Notices of the RAS*, **526**, 2830, DOI: 10.1093/mnras/stad2759
- Foreman-Mackey, D., Luger, R., Agol, E., et al., exoplanet: Gradient-based probabilistic inference for exoplanet data & other astronomical time series. 2021, *The Journal of Open Source Software*, **6**, 3285, DOI: 10.21105/joss.03285
- Fortney, J. J., Shabram, M., Showman, A. P., et al., Transmission Spectra of Three-Dimensional Hot Jupiter Model Atmospheres. 2010, *Astrophysical Journal*, **709**, 1396, DOI: 10.1088/0004-637X/709/2/1396
- Gajdoš, P. & Parimucha, Š., New tool with GUI for fitting O-C diagrams. 2019, *Open European Journal on Variable Stars*, **197**, 71
- Garai, Z., Pribulla, T., Komžík, R., et al., Periodic transit timing variations and refined system parameters of the exoplanet XO-6b. 2020, *Monthly Notices of the RAS*, **491**, 2760, DOI: 10.1093/mnras/stz3235

- Hayward, T. L., Brandl, B., Pirger, B., et al., PHARO: A Near-Infrared Camera for the Palomar Adaptive Optics System. 2001, *Publications of the ASP*, **113**, 105, DOI: 10.1086/317969
- Howell, S. B., Everett, M. E., Horch, E. P., et al., Speckle Imaging Excludes Low-mass Companions Orbiting the Exoplanet Host Star TRAPPIST-1. 2016, *Astrophysical Journal, Letters*, **829**, L2, DOI: 10.3847/2041-8205/829/1/L2
- Howell, S. B. & Furlan, E., Speckle Interferometric Observations With the Gemini 8-m Telescopes: Signal-to-Noise Calculations and Observational Results. 2022, *Frontiers in Astronomy and Space Sciences*, **9**, DOI: 10.3389/fspas.2022.871163
- Jensen, E. 2013, Tapir: A web interface for transit/eclipse observability, Astrophysics Source Code Library, record ascl:1306.007
- Kabáth, P., Chaturvedi, P., MacQueen, P. J., et al., TOI-2046b, TOI-1181b, and TOI-1516b, three new hot Jupiters from TESS: planets orbiting a young star, a subgiant, and a normal star. 2022, *Monthly Notices of the RAS*, **513**, 5955, DOI: 10.1093/mnras/stac1254
- Kipping, D. M., Efficient, uninformative sampling of limb darkening coefficients for two-parameter laws. 2013, *Monthly Notices of the RAS*, **435**, 2152, DOI: 10.1093/mnras/stt1435
- Kokori, A., Tsiaras, A., Edwards, B., et al., ExoClock project: an open platform for monitoring the ephemerides of Ariel targets with contributions from the public. 2022, *Experimental Astronomy*, **53**, 547, DOI: 10.1007/s10686-020-09696-3
- Kovács, G., Zucker, S., & Mazeh, T., A box-fitting algorithm in the search for periodic transits. 2002, *Astronomy and Astrophysics*, **391**, 369, DOI: 10.1051/0004-6361:20020802
- Lambert, M., Bender, C. F., Kanodia, S., et al., TOI-5375 B: A Very Low Mass Star at the Hydrogen-burning Limit Orbiting an Early M-type Star. 2023, *Astronomical Journal*, **165**, 218, DOI: 10.3847/1538-3881/acc651
- Lightkurve Collaboration, Cardoso, J. V. d. M., Hedges, C., et al. 2018, Lightkurve: Kepler and TESS time series analysis in Python, Astrophysics Source Code Library, record ascl:1812.013
- Mesarč, M. 2023, Validation of selected *TESS* exoplanetary candidate
- Morello, G., Claret, A., Martin-Lagarde, M., et al., The ExoTETHyS Package: Tools for Exoplanetary Transits around Host Stars. 2020, *Astronomical Journal*, **159**, 75, DOI: 10.3847/1538-3881/ab63dc
- Narita, N., Fukui, A., Kusakabe, N., et al., MuSCAT2: four-color simultaneous camera for the 1.52-m Telescopio Carlos Sánchez. 2019, *Journal of Astronomical Telescopes, Instruments, and Systems*, **5**, 015001, DOI: 10.1117/1.JATIS.5.1.015001
- Poddaný, S., Brát, L., & Pejcha, O., Exoplanet Transit Database. Reduction and processing of the photometric data of exoplanet transits. 2010, *New Astronomy*, **15**, 297, DOI: 10.1016/j.newast.2009.09.001

- Ricker, G. R., Winn, J. N., Vanderspek, R., et al., Transiting Exoplanet Survey Satellite (TESS). 2015, *Journal of Astronomical Telescopes, Instruments, and Systems*, **1**, 014003, DOI: 10.1117/1.JATIS.1.1.014003
- Safonov, B. S., Lysenko, P. A., & Dodin, A. V., The speckle polarimeter of the 2.5-m telescope: Design and calibration. 2017, *Astronomy Letters*, **43**, 344, DOI: 10.1134/S1063773717050036
- Tingley, B., Using color photometry to separate transiting exoplanets from false positives. 2004, *Astronomy and Astrophysics*, **425**, 1125, DOI: 10.1051/0004-6361:20035792
- Tsiaras, A., HOPS: the photometric software of the HOlomon Astronomical Station. in , *EPSC-DPS joint Meeting - Exoplanet exploration*, Vol. **13**, EPSC–DPS2019–1594
- Tsiaras, A., Waldmann, I. P., Rocchetto, M., et al. 2016, pylightcurve: Exoplanet lightcurve model, Astrophysics Source Code Library, record ascl:1612.018
- Wong, I., Shporer, A., Zhou, G., et al., TOI-2109: An Ultrahot Gas Giant on a 16 hr Orbit. 2021, *Astronomical Journal*, **162**, 256, DOI: 10.3847/1538-3881/ac26bd